NASA/TM—2016-219081

Altitude Effects on Thermal Ice Protection System Performance; a Study of an Alternative Approach

Harold E. Addy, Jr.
Glenn Research Center, Cleveland, Ohio

David Orchard
National Research Council Canada, Ottawa, Canada

William B. Wright
Vantage Partners, LLC, Cleveland, Ohio

Myron Oleskiw
National Research Council Canada, Ottawa, Canada

May 2016

NASA STI Program . . . in Profile

Since its founding, NASA has been dedicated to the advancement of aeronautics and space science. The NASA Scientific and Technical Information (STI) Program plays a key part in helping NASA maintain this important role.

The NASA STI Program operates under the auspices of the Agency Chief Information Officer. It collects, organizes, provides for archiving, and disseminates NASA's STI. The NASA STI Program provides access to the NASA Technical Report Server—Registered (NTRS Reg) and NASA Technical Report Server—Public (NTRS) thus providing one of the largest collections of aeronautical and space science STI in the world. Results are published in both non-NASA channels and by NASA in the NASA STI Report Series, which includes the following report types:

- TECHNICAL PUBLICATION. Reports of completed research or a major significant phase of research that present the results of NASA programs and include extensive data or theoretical analysis. Includes compilations of significant scientific and technical data and information deemed to be of continuing reference value. NASA counter-part of peer-reviewed formal professional papers, but has less stringent limitations on manuscript length and extent of graphic presentations.

- TECHNICAL MEMORANDUM. Scientific and technical findings that are preliminary or of specialized interest, e.g., "quick-release" reports, working papers, and bibliographies that contain minimal annotation. Does not contain extensive analysis.

- CONTRACTOR REPORT. Scientific and technical findings by NASA-sponsored contractors and grantees.

- CONFERENCE PUBLICATION. Collected papers from scientific and technical conferences, symposia, seminars, or other meetings sponsored or co-sponsored by NASA.

- SPECIAL PUBLICATION. Scientific, technical, or historical information from NASA programs, projects, and missions, often concerned with subjects having substantial public interest.

- TECHNICAL TRANSLATION. English-language translations of foreign scientific and technical material pertinent to NASA's mission.

For more information about the NASA STI program, see the following:

- Access the NASA STI program home page at http://www.sti.nasa.gov

- E-mail your question to help@sti.nasa.gov

- Fax your question to the NASA STI Information Desk at 757-864-6500

- Telephone the NASA STI Information Desk at 757-864-9658

- Write to:
  NASA STI Program
  Mail Stop 148
  NASA Langley Research Center
  Hampton, VA 23681-2199

NASA/TM—2016-219081

Altitude Effects on Thermal Ice Protection System Performance; a Study of an Alternative Approach

Harold E. Addy, Jr.
Glenn Research Center, Cleveland, Ohio

David Orchard
National Research Council Canada, Ottawa, Canada

William B. Wright
Vantage Partners, LLC, Cleveland, Ohio

Myron Oleskiw
National Research Council Canada, Ottawa, Canada

National Aeronautics and
Space Administration

Glenn Research Center
Cleveland, Ohio 44135

May 2016

Acknowledgments

The authors would like to express their great appreciation to Gislain Chevrette and Steve Totolo at National Research Council Canada's Altitude Icing Wind Tunnel for model installation and test operations; to Bill Magus, Paul Butterfield, and Terry Mathes at NASA's Icing Research Tunnel for model check out; and Sharon Lewis at NASA's Shipping and Receiving department for coordinating model shipment and customs clearance.

Level of Review: This material has been technically reviewed by technical management.

Available from

NASA STI Program
Mail Stop 148
NASA Langley Research Center
Hampton, VA 23681-2199

National Technical Information Service
5285 Port Royal Road
Springfield, VA 22161
703-605-6000

This report is available in electronic form at http://www.sti.nasa.gov/ and http://ntrs.nasa.gov/

Altitude Effects on Thermal Ice Protection System Performance; a Study of an Alternative Approach

Harold E. Addy, Jr.
National Aeronautics and Space Administration
Glenn Research Center
Cleveland, Ohio 44135

David Orchard
National Research Council Canada
Ottawa, Canada

William B. Wright
Vantage Partners, LLC
Cleveland, Ohio 44135

Myron Oleskiw
National Research Council Canada
Ottawa, Canada

Abstract

Research has been conducted to better understand the phenomena involved during operation of an aircraft's thermal ice protection system under running wet icing conditions. In such situations, supercooled water striking a thermally ice-protected surface does not fully evaporate but runs aft to a location where it freezes. The effects of altitude, in terms of air pressure and density, on the processes involved were of particular interest. Initial study results showed that the altitude effects on heat energy transfer were accurately modeled using existing methods, but water mass transport was not. Based upon those results, a new method to account for altitude effects on thermal ice protection system operation was proposed. The method employs a two-step process where heat energy and mass transport are sequentially matched, linked by matched surface temperatures. While not providing exact matching of heat and mass transport to reference conditions, the method produces a better simulation than other methods. Moreover, it does not rely on the application of empirical correction factors, but instead relies on the straightforward application of the primary physics involved. This report describes the method, shows results of testing the method, and discusses its limitations.

Nomenclature

c	model chord
d	twice the model leading edge radius
IPS	ice protection system
K	inertia parameter
K_0	modified inertia parameter
LWC	liquid water content
M	Mach number
MVD	median volumetric diameter
M_w	water loading
Pr	Prandtl number

qdot	power density
r	recovery factor
Re	Reynolds number
Re_{cl}	Reynolds number based on droplet diameter
s	surface distance
T_r	recovery temperature
T_{st}	static temperature
T_t	total temperature
V_{tas}	true air speed
γ	ratio of specific heats for air
μ_{air}	air viscosity
ρ_{air}	air density
ρ_w	water density
σ_{wa}	surface tension, water-air
β_0	collection efficiency at stagnation
λ/λStokes	droplet range parameter
δ	droplet median volumetric diameter

Introduction

The energy required to operate an aircraft's thermal ice protection system (IPS) can be considerable. As new aircraft are being designed for higher efficiencies, all energy-consuming systems on the aircraft are being re-examined with the goal of reducing their energy needs. One way to reduce energy requirements of a thermal IPS is to design it to operate in a 'running wet' mode under more extreme icing conditions. In a running wet mode, the water impinging on the protected surface is warmed only enough to allow it to run completely off the aircraft or back to a noncritical area before freezing. This requires significantly less energy than operating in a mode where all the impinging water is evaporated.

The running wet mode of operation, however, requires that energy requirements be more accurately calculated and evaluated. These energy requirements must account for the many aspects of the aircraft icing process including air temperature, air speed, cloud water content, as well as aircraft altitude. Much research and development of thermal ice protection systems is done in atmospheric icing wind tunnels that cannot simulate the altitude affects to a meaningful extent. Therefore, the effects of altitude on thermal IPS operation must be approximated using scaling techniques. Various methods of scaling for altitude effects have been proposed and used, but a vigorous validation so as to produce a widespread acceptance of any one of them has not been achieved. A better understanding of the processes involved in thermal IPS operation at altitude is needed to develop a validated and more widely accepted altitude scaling method. This, in turn, will enable more exact design, testing, and evaluation of these systems.

In order to address the issues associated with altitude effects on thermal IPS operation, the National Aeronautics and Space Administration (NASA) and the National Research Council Canada (NRCC) entered into an agreement to jointly study the problem. It is the first such study conducted specifically to better understand the effects of altitude on the heat and mass transfer processes occurring during operation of a thermal IPS in flight icing conditions with the intent to make the results publicly available. NRCC provided test time in the Altitude Icing Wind Tunnel (AIWT) in Ottawa, Canada for two separate campaigns: one in 2012 and one in 2014. The AIWT produces aircraft inflight icing conditions over a range of air speeds, temperatures, and pressure altitudes as well as inflight icing cloud densities and droplet sizes. NASA provided a NACA airfoil model equipped with a piccolo tube heated-air IPS. The

model was instrumented such that heated-air flow rates and temperatures could be measured and inner surface temperatures of the model's leading edge could be monitored.

During the initial AIWT campaign in 2012, an altitude scaling technique based upon heat transfer, droplet impingement, water loading, and recovery temperature similarity was used to help better understand the processes involved and to identify primary test parameters. Results from the initial campaign were used to develop a new altitude scaling method which was investigated during the second AIWT campaign. The development of the new altitude scaling method along with results from the second AIWT campaign are discussed in this report.

Background

Altitude Scaling—Initial Campaign

The method used for the initial AIWT campaign to scale test conditions so as to achieve similarity between altitude and ground level was based largely on a method that has some acceptance in the aviation industry (Ref. 1). Briefly, the method identifies four key scaling parameters and then other test conditions are varied so as to keep the four key parameters constant between altitude and ground level. The four key parameters are: Reynolds number, water loading, inertia parameter, and recovery temperature. These parameters are described in further detail below.

A thermal IPS's use of heat energy to inhibit or prevent the buildup of ice on an aircraft surface obviously makes heat transfer a primary parameter in its operation. Part of that heat energy is transferred to the cold air flowing over the aircraft surface. Empirical analysis of thermal IPS operation has most often found that the heat transfer coefficient is typically a function of the external Reynolds number. It follows then, that to obtain similar results at altitude and ground level, the external Reynolds number must be the same for both reference and scale cases. The following expression for Reynolds number was applied (Ref. 2):

$$\mathrm{Re} = \frac{\rho_{\mathrm{air}} \cdot V_{\mathrm{tas}} \cdot d}{\mu_{\mathrm{air}}} \tag{1}$$

Heat energy is also transferred to the supercooled liquid water droplets striking the surface to prevent freezing. The amount of heat energy required for this purpose is a function of, among other parameters, the amount of water collecting, or water loading, on the aircraft surface. To reduce the complications involved with scaling this aspect of thermal IPS operation, the common approach is to maintain the water loading at the same level for both the altitude and ground level conditions. The following expression for water loading was used (Ref. 2):

$$M_{\mathrm{w}} = \mathrm{LWC} \cdot V_{\mathrm{tas}} \cdot \beta_0 \tag{2}$$

The coverage area of the impinging water should also be the same between altitude and ground level. This was achieved by matching the modified droplet inertia parameter (Ref. 2):

$$K_0 = \frac{1}{8} + \frac{\lambda}{\lambda_{\mathrm{Stokes}}}\left(K - \frac{1}{8}\right) \tag{3}$$

where:

$$K = \frac{\rho_w \cdot \delta^2 \cdot V_{\text{tas}}}{18 d \mu_{\text{air}}} \tag{4}$$

and for air:

$$\frac{\lambda}{\lambda_{\text{Stokes}}} = \frac{1}{0.8388 + 0.001483 \text{Re}_\delta + 0.1847 \sqrt{\text{Re}_\delta}} \tag{5}$$

Air temperature also plays a major role in the heat energy transfer. Because matching external Reynolds number between altitude and ground level conditions results in very different airspeeds for the two, it then follows that both total air temperature and static air temperature cannot be matched. For unprotected surfaces, total air temperature is a driving factor, with static air temperature playing a lesser role. In a running wet situation, where the ice forms further aft on the airfoil, static air temperature may play a greater role. Recovery temperature lies between static and total temperature. It is the temperature an adiabatic wall aligned with the air flow will reach in steady flow. While an adiabatic wall does not occur with a thermal IPS, the use of a calculated recovery temperature provides a practical temperature for setting scaled icing conditions that is between total and static temperatures. Here, the recovery temperature is calculated by:

$$T_r = T_{st} \left(1 + r \left(\frac{\gamma - 1}{2} \right) M^2 \right) \tag{6}$$

where:

$$r = \sqrt{Pr}$$

In addition to the heat energy transfer, mass transport is occurring in the form of water striking the airfoil and running aft on its surface. Some of the water is evaporated, while some freezes on the airfoil surface after running some distance downstream of the leading edge. In this situation, conditions are such that the Reynolds analogy or, more specifically, the Chilton-Colburn analogy (Ref. 3), should apply. Therefore, by similarity, the mass transfer coefficient should be a function of the heat transfer coefficient. Both heat and mass transfer coefficients, then, should be dependent on Reynolds number. This forms the basis for use of Reynolds number matching for the scaling of test conditions between altitude and ground level testing.

Test Results—Initial Campaign

In the initial test, the thermal IPS scaling method described above was investigated using the altitude capability of the NRC's AIWT along with a specially designed airfoil and thermal IPS model provided by NASA. In addition to the investigation of the thermal IPS scaling method, the model design allowed for a more careful observation of the phenomena involved.

For the test, three different icing flight scenarios where selected as the reference (altitude) conditions and corresponding scale (ground-level) conditions and calculated using the scaling method. The three scenarios were designated: Warm Hold, Cold Hold, and Descent. The scenario designations described three different aircraft icing scenarios where an aircraft might likely be operating a running-wet mode. Warm Hold refers to conditions where the icing cloud is at a temperature below, but near freezing and at a relatively high liquid water content (LWC). Cold Hold is a set of icing conditions where the cloud temperature is near the lower range where liquid water droplets can remain unfrozen. Here, the LWC is lower than in the Warm Hold scenario. The Descent condition is mid-range in both temperature and LWC, but is a phase of aircraft flight where less heat energy is available onboard. Results of the tests were compared using photographs, tracings, and mass measurements of the accreted ice. In addition, measurements were made of airfoil surface temperatures and thermal IPS heat energy used.

The reader is referred to Reference 4 for a detailed description of the initial test campaign and its results. In summary, however, the tests showed:

(1) Airfoil surface temperatures and thermal IPS heat energy use were well matched between altitude and corresponding ground-level conditions. This comparison was particularly good for dry-air conditions where the icing cloud was not activated but Reynolds-number matching dictated differing air speeds and air temperatures. The comparison was also very good for the wet-air conditions where the icing cloud was activated, but not as close as the dry-air conditions. The mass transport of water complicates the situation quite a bit. Water loading, water runback, and water evaporation were all at play.

(2) For two of the three scenarios, Warm Hold and Descent, the amount of ice accreted as well as its location on the airfoil was not well matched. For these scenarios, more ice was accreted at the ground-level cases and it froze further aft on the airfoil surface. The Cold Hold results were somewhat inconclusive because difficulties during the test complicated execution of the reference and scale cases for this scenario and other test priorities and limitations precluded the repeating the cases. Other complications arose in setting icing conditions in the tunnel for the Warm Hold and Descent scenarios which resulted in more uncertainty than was expected. The differences in the ice accretions for these scenarios were, however, more than could be explained by the increased uncertainty. The differences in ice mass and location were so pronounced that it was clear that the thermal IPS scaling method used was inadequate and unable to be effectively employed to accurately predict runback ice accretion when testing at ground-level conditions for at least a considerable range of flight scenarios.

(3) During running-wet thermal IPS operation, water flowed aft in the form of drops and rivulets to areas where conditions permitted freezing. In these areas, both ice and liquid water were observed with the liquid water in the form of drops on top of the ice. Periodically, the drops would disappear. Instead of entirely evaporating or freezing in place, water may have been being re-entrained in the air flow. Such water transport had not been considered in the scaling method.

Development of Alternative Scaling Method

Water Droplet Entrainment

The degree of runback water behavior observed during the initial test campaign strongly indicated that further investigation of this aspect of the running-wet mode of operation for a thermal IPS was needed. A review of literature related to this type of phenomenon yielded a number of references pertinent to the topic. Various studies of water drop entrainment into gaseous flows have been conducted (Refs. 5 to 7). Weber number, a measure of inertia forces relative to surface tension forces, is a key parameter in describing the phenomena. In addition, Olsen and Walker (Ref. 8) noted the significance of water drop movement on the surface of ice in aircraft icing conditions where the incoming water did not freeze on impact. Studies by Kind and Oleskiw (Ref. 9) and by Feo (Ref. 10) also investigate and

recognize the significance of surface water movement in aircraft icing. The analysis prior to the initial test in this study recognized that Weber number was not being matched in the scaling method used. In scaling aircraft icing conditions for the effects of altitude, it is not feasible, if not impossible, to simultaneously match both Reynolds number and Weber number. Because the rate of water re-entrainment into the airstream was not considered significant, Reynolds number was determined to be the more important parameter to match.

Experience gained through the initial tests indicated that matching Weber numbers between reference and scale was worthy of investigation. There are, however, different variations of the Weber number where different characteristic velocities, densities, and lengths have been used. For this phase of the study, Weber based on air speed, density of water, and leading edge diameter was selected as this version showed best correlation with ice mass lost in the first series of tests at AIWT.

Application of Weber Number

The Weber number used here takes the form of:

$$We = \frac{\rho_w \cdot V^2_{tas} \cdot d}{\sigma_{wa}} \tag{7}$$

Neither the density of water nor the water-air surface tension vary as a function of altitude and the same airfoil model was used throughout, so *d*, twice the model leading edge radius, also remained constant. Weber number, then, is matched between altitude and ground-level by matching airspeed. Because Reynolds number is a function of both airspeed and air density, however, matching airspeed means that Reynolds number is not matched. Matching Weber number yields a Reynolds number that is much higher at ground-level than at altitude conditions. This means that heat transfer from the airfoil surface to the exterior airflow is much higher that at altitude, or reference condition. With higher heat transfer rates, lower airfoil surface temperatures and more freezing of runback ice would be expected.

A way to counter the elevated convection that occurs at Weber number scaled conditions is to increase the heat energy provided by the thermal IPS. This can be done by increasing the thermal IPS air temperature and/or flowrate so as to match the airfoil leading edge surface temperatures when operating at ground-level conditions as determined by Reynolds number scaling. As indicated earlier in this report, the initial tests in this study showed that Reynolds number scaling produces surface temperatures that are closely matched between altitude and ground level. While still not providing matching heat transfer rates, providing matching surface temperatures is an important step in achieving ice accretion similarity.

This scaling process, then, requires two steps: (1) a test run with Reynolds number scaling to achieve heat transfer similarity and, therefore, surface temperatures for use in the second step and (2) a test run with Weber number scaling to get ice accretion similarity with a reset thermal IPS to obtain the surface temperatures of the first step. The Weber scaling step assumes water re-entrainment is a major contributor to the difference in accreted ice between reference and Reynolds number scaled conditions as was seen in the initial tests. For each step, scaling of water loading, inertia parameter, and recovery temperature are done to ensure similarity of these parameters to the reference conditions. They have no significant effect on either Reynolds or Weber numbers.

Second AIWT Campaign Objectives

The objectives of the second campaign in the AIWT were threefold: (1) employ Weber number scaling as a method to help establish the validity of the water re-entrainment hypothesis, (2) verify results of the first AIWT campaign, and (3) develop a further understanding of the processes involved in runback ice accretion. Similar to the initial AIWT campaign, three flight scenarios where runback icing might occur were selected for the reference conditions. These scenarios were then scaled for ground-level testing using Weber number-based scaling as described above. Similarity of runback ice accretions

between altitude and ground-level would be considered an indication of the validity of the water re-entrainment hypothesis. Test points would also be run at ground-level using Reynolds number-based scaling as in the first AIWT campaign. This would help verify the results of the initial campaign, where some discrepancy between planned test points and actual run conditions were later discovered. Finally, high-speed, high-resolution videography was used for a portion of the test to better observe the behavior of water rivulets and water droplets on the airfoil surface during runback icing.

Test Plan

Icing Scenarios

As in the initial AIWT campaign, a set of icing conditions were selected to approximate three different aircraft icing scenarios at altitude: an aircraft hold at relatively low icing air temperature (Cold Hold), a hold at relatively warm icing temperature (Warm Hold), and a descent at intermediate icing temperature (Descent). These conditions are given in Table 1 and will be referred to as reference conditions. IPS heated air flow rates and temperatures were set to provide a 'running wet' mode of operation for the ice protection. In this mode, not all the water impinging on the leading edge of the model is evaporated. Some flows aft on the aircraft surface before freezing in an area that is presumably less critical to the model's aerodynamics. For the purposes of this study, however, aerodynamic criticality was not a primary consideration. Instead, better understanding the heat and mass transfer phenomena involved in the accretion of ice in conjunction with a heat source (a thermal IPS), was the focus.

The test plan also included runs without the IPS operating. These runs provided data in terms of unprotected ice accretion shapes and masses that could be used for post-test analysis and comparison purposes.

Scaling for Ground Level

In addition to the three aircraft icing scenarios at altitude, corresponding icing conditions at ground level using both Reynolds number based and Weber number based scaling methods were selected for the test. These conditions were calculated as described above. The Reynolds number and Weber number scaled conditions for each of the three flight scenarios along with the corresponding conditions at altitude (reference) are given in Table 2. In addition to the cloud conditions, the Reynolds number, Weber number, water loading, inertia parameter, and recovery temperature are shown in Table 2. For all test points, the model was set at an angle of attack of 0°.

TABLE 1.—REFERENCE CONDITIONS

Flight phase	Altitude, ft	V_{tas}, kts	AOA, degree	T_{st}, °C	LWC, g/m^3	MVD, μm
Cold hold	15000	180	0	–30	0.24	20
Warm hold	15000	180	0	–9	0.50	20
Descent	10000	180	0	–14	0.35	20

TABLE 2.—REFERENCE AND CORRESPONDING SCALE CONDITIONS

Flight phase	Alt., m	V, kts	T_{st}, °C	LWC, g/m^3	MVD, μm	Re_d ×10^6	We_d ×10^6	M_w g/m^2-s	K_0	T_r, °C
Descent(ref)	3050	180	–14	0.35	19.6	1.58	4.30	20.3	1.37	–10
(Re sc)		130	–12	0.49	24.0	1.58	2.24	20.3	1.37	–10
(We sc)		180	–14	0.35	21.1	2.15	4.30	20.3	1.37	–10
Cld Hld(ref)	4570	180	–30	0.24	17.4	1.43	4.30	13.4	1.23	–26
(Re sc)		106	–28	0.41	24.2	1.43	1.40	13.4	1.23	–26
(We sc)		180	–30	0.24	19.5	2.35	4.30	13.4	1.23	–26
Wm Hld(ref)	4570	180	–8	0.54	17.7	1.26	4.30	30.3	1.24	–5
(Re sc)		106	–6	0.91	24.5	1.26	1.50	30.3	1.24	–5
(We sc)		180	–8	0.54	19.8	2.08	4.30	30.3	1.24	–5

Facility Description

The AIWT is a specialized closed-loop, low to moderate speed wind tunnel used to simulate in-flight atmospheric icing conditions. The tunnel's standard test section is 22.5 $in.^2$ and 6 ft long. The airspeed in this test section can vary from about 10 to 195 kts. Access panels in the tunnel walls, floor and ceiling provide rapid access to test articles as well as flexibility in their mounting in the test section. Plexiglas windows are commonly installed in the test section to enable photographic or video recording of ice formation and growth. Airspeed in the tunnel is computer-controlled using a variable frequency drive which provides power to the fan's 600 hp motor. Test section flow uniformity and a relatively low turbulence level are enhanced through the use of a honeycomb structure and screen at the entry of the settling chamber.

A heat exchanger located upstream of the tunnel's settling chamber permits rapid changes of air temperature within the test section. The use of a three-way valve to control the flow of chilled trichloroethylene through the heat exchanger permits a high level of temporal stability of air temperature in the tunnel. The closed cell insulation surrounding the tunnel shell assists in the ability to obtain static air temperatures as low as –30 °F (–34.4 °C). A thick steel tunnel shell combined with the operation of vacuum pumps permits partial evacuation of the air from the tunnel to simulate flight at altitudes as high as 30,000 ft.

Six spray bars are located at the entry to the settling chamber, just downstream of the turbulence-reduction screens. Up to 5 of 7 spray nozzles in each spray bar may be selected at any one time in various patterns to ensure adequate spray coverage across the test section. By varying the flow rate of distilled water to the external-mix spray nozzles, the liquid water content (LWC) in the test section may be varied between 0.1 and 3.0 g/m^3. Controlling the spray air pressure permits the median volumetric diameter (MVD) of the spray droplet size distribution to vary between 10 and 200 μm. Additional details regarding the tunnel are provided in Oleskiw et al. (Ref. 11).

Model Description

The airfoil model used for both the initial campaign as well as the campaign described in this report was an 18-in. chord NACA-0018. A symmetric airfoil was selected for this fundamental study primarily because it reduces the number of complicating factors in the test. Its 18-in. chord length was chosen so that the model would fit it the AIWT test section without undue difficulty or complications. The relatively thick airfoil was chosen to provide a wider leading edge which allowed more space for installation of a thermal IPS and measurement instruments inside. This 2D, straight wing model spanned the 22.5 in. wide AIWT from wall to wall. It was constructed of a 0.063 in. thick 7075-T6 aluminum skin on a 0.625 in. thick 7075 aluminum rib and spar frame. The trailing edge was also machined from 7075 aluminum.

A heated-air piccolo tube IPS was designed for the model. The primary objective of the design was to provide a 2D heating system with minimal span-wise variation in the temperature and heat transfer profiles during testing. This would simplify modeling and analysis of the measurements. For these reasons, the forward edge of the full-span piccolo tube was located 1.25 in. from the inside of the leading edge and had a single, straight row of 42, 0.032-in. diameter holes spaced 31/64 in. apart. A steel diffuser was designed to direct the heated airflow to and around the inside of the leading edge. Four aluminum ribs were used to maintain the diffuser shape. A cross section of the leading edge of the airfoil showing the IPS design is shown in Figure 1.

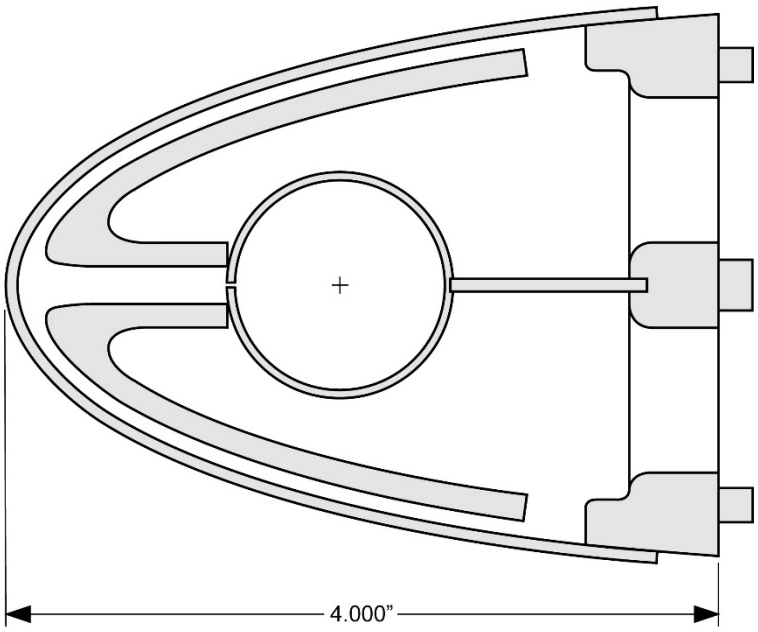

Figure 1.—Model leading edge cross section.

Heated air was supplied to one end of the piccolo tube where it was directed to the inner surface of the leading edge via small holes. The heated air was then directed along the inner surface of the leading edge by a symmetric diffuser. The heated air exited the model through exhaust pipes mounted to a spar at the aft of the leading edge. The heated exhaust air flowing from the upper surface was kept separate from that flowing from the lower surface by a horizontal wall extending from the aft of the piccolo tube to the spar. Each of these two exhaust flows were measured by a Coriolis flow meter located in the respective exhaust pipe. Manual valves situated downstream of the flow meters were adjusted to ensure proper flow rates maintained equal heating to both the upper and lower surfaces of the leading edge.

Thermocouples were used to measure model surface and heated air temperatures. On the inner surface of the leading edge, thin film (0.0005 in. thick), T-type thermocouples were installed using a thin layer (approximately 0.002 in. thick) of thermally-conductive epoxy (M-Bond). This method of installation minimizes the difference between the measurement and the surface temperature. The difference was estimated to be well within the measurement uncertainty.

Three T-type thermocouples were used to monitor the temperature of the heated air flowing into the model. One was at the entrance to the piccolo tube while two were spaced axially along the center of the tube using a rod device that was inserted into the end of the piccolo tube. Heated air exhaust temperatures were measured using six T-type thermocouples mounted through the front spar of the model. Further details of the model and measurement instruments are given in Reference 3.

Test Procedure

The test was designed to be run in a sequence of steps for each of the three flight scenarios. First, the tunnel was run at the reference icing conditions while the IPS settings (temperature and flowrate) were adjusted to obtain runback ice accretion. The test point at reference conditions was then run for a set period of time using the IPS settings determined during the previous step. Test runs were then made, in turn, for the Reynolds number and Weber number scaled test points.

The IPS settings for the Reynolds-scaled test point were the same as those used for the reference run, to ensure the same heat energy input was used. These data points were used to help verify the results from the initial AIWT campaign and to provide direct comparison data for the Weber number scaled tests.

For the Weber number scaled test points, the tunnel airspeed and temperature were brought to the planned values. Then the thermal IPS settings were adjusted to obtain the same, or nearly the same, model leading edge surface temperatures as were obtained in the reference test run. The icing cloud was then activated to complete the test point.

At the conclusion of each test run, photographs were taken of the accreted ice. For ice accretions that had formed a spanwise ridge on the leading edge of the model, ice tracings were made at the model centerline to record the shape and location of the ice. For ice accretions that had formed frozen runback rivulets aft of the model leading edge, an impression of the ice on the upper surface was made using a block of impression foam. These impression blocks could be scanned later using a 3D laser scanner. Ice depth measurements were also made and then the ice was removed from the model and weighed. The ice mass values reported are for the ice accreted over the center 10.5 in. of the model. Results of the tests will be discussed in terms of these measurements as well as the model leading edge temperatures and heated air flow rates and temperatures.

Model and heated air thermocouples were calibrated before the tests and were found to be within ±1 °C. The heated air flow meters were recalibrated before the tests and were found to be accurate to ±1 percent. Three thermocouples measuring leading edge surface temperatures were, however, damaged during model assembly and did not yield accurate measurements. Difficulties with the thermocouple data acquisition system lead to erroneous measurements from five more leading edge surface thermocouples. All eight of these temperature measurements have been removed from the data analysis and the plots presented in this report. The error in ice depth and mass measurements can only be approximated due to ergonomic challenges. Repeat measurements of ice accreted without the IPS operating indicated that they were likely to be within ±10 percent.

Results

Descent Case

Figures 2(a) to (c) show photographs of ice accreted on the lower surface of the model for the reference, Reynolds number scaled, and Weber number scaled conditions for the Descent case. Qualitatively, the ice shapes are similar. This similarity is reflected in the mid-span ice tracings shown in Figure 3. The tracings do, however, show that more ice was accreted at the Reynolds number scaled conditions and that it froze slightly further aft on the model. The measured masses of ice and the height of the ice on both the upper and lower surfaces for reference and scaled conditions are given in Table 3.

Figure 2.—Descent case (a) Reference, (b) Reynolds scaling, and (c) Weber scaling.

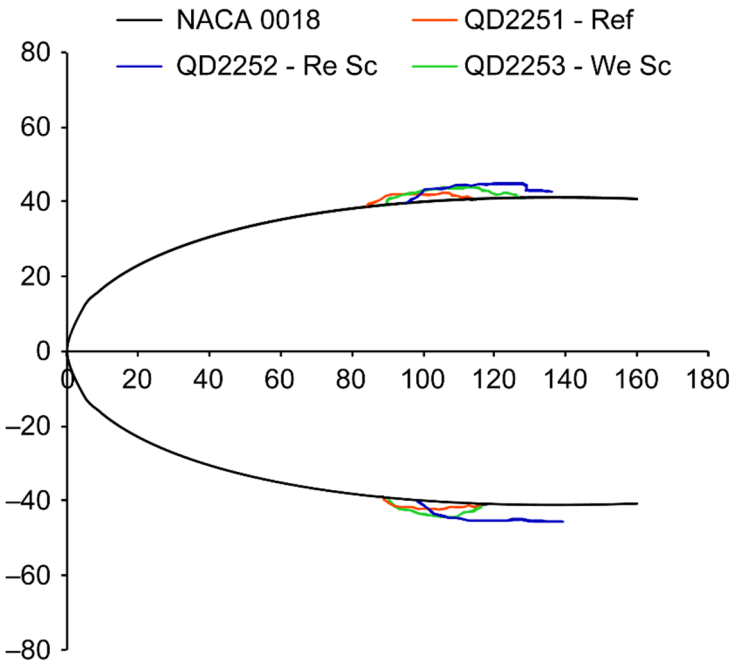

Figure 3.—Descent ice tracings.

TABLE 3.—DESCENT CASE RESULTS

Flight phase	Alt., m	V_{tas}, kts	T_{st}, °C	T_t, °C	LWC, g/m^3	MVD, μm	Tau, s	Up ice, in.	Lo ice, in.	Ice mass, g
Descent (ref)	3050	180	–14.1	–9.9	0.38	19.5	600	0.28	0.30	33
(Re sc)	453	130	–12.4	–10.2	0.50	24.3	600	0.17	0.19	57
(We sc)	775	180	–14.2	–9.9	0.36	21.5	600	0.14	0.23	31

Figure 4 shows the model surface temperatures during the runs both before exposing the model to the cloud (dry) and again during exposure to the cloud (wet). The close agreement between reference and Reynolds number scaled in the dry conditions indicate the degree to which matching Reynolds number matches heat transfer between the two. For the Weber number scaled run, the IPS settings were adjusted to obtain dry surface temperatures that matched those of the reference run. These temperatures could not be matched perfectly around the leading edge as the heat transfer rates differ under the Weber number scaled conditions.

There is slightly more difference between the surface temperatures in the wet conditions. Increased surface cooling was observed during the wet reference conditions. This is likely due to an increase in evaporative cooling at the lower tunnel air pressure of the reference conditions.

The measured reference and scale IPS heated air inlet and outlet temperatures for both the dry and wet conditions for this case are shown in Figure 5(a). The heat energy used by the IPS is shown in Figure 5(b). As in the initial AIWT campaign, there was close agreement between reference and Reynolds number scaled values for these parameters indicating the heat transfer characteristics at altitude are closely matched using Reynolds number based scaling. As expected, the heat transfer is elevated at the Weber number scaled conditions.

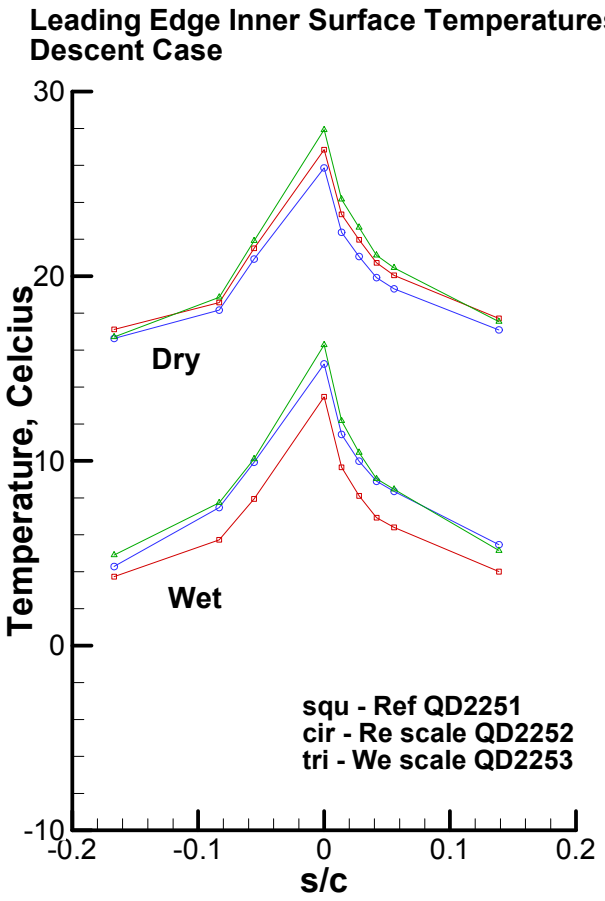

Figure 4.—Descent surface temperatures before (dry) and during (wet) exposure to icing cloud.

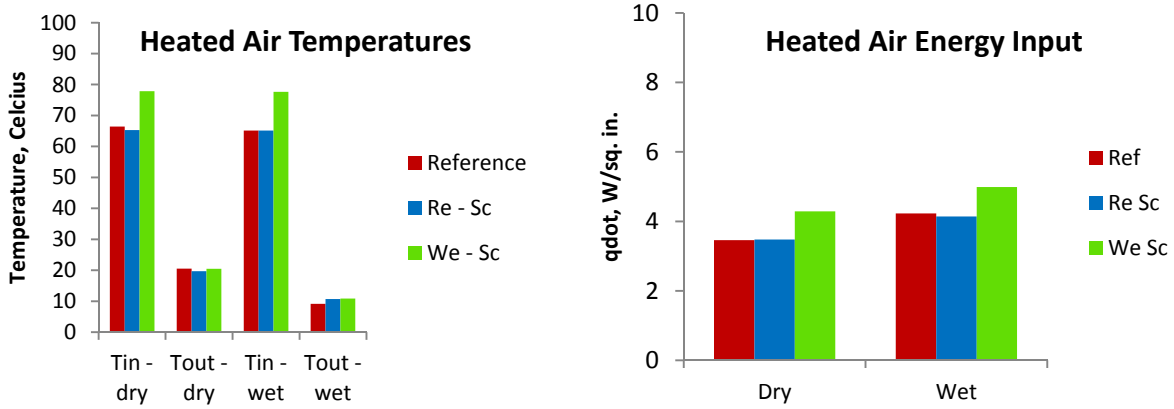

Figure 5.—Descent (a) heated air temperatures and (b) heated air energy input before and during exposure to icing cloud.

Warm Hold Case

Photographs of the ice accreted at the reference, Reynolds number scaled, and Weber number scaled conditions for the Warm Hold case are shown in Figures 6(a) to (c), respectively. The type of ice formed in all three cases is similar, but there is much more ice accreted for the Reynolds number scaled case than in the other two cases. It is located further aft on the airfoil and extends over a much greater distance in the chordwise direction, although its thickness is similar to that for the Weber number scaled run. The ice accreted further aft on the model than in the other scenarios such that its profile could not be recorded using the tracing templates, so impressions of the ice were made using the foam blocks. Images from the 3D scans of the impressions in the blocks of the ice accretions from the upper surface of the model are shown in Figure 7. The ice depth and mass data for this case are shown in Table 4.

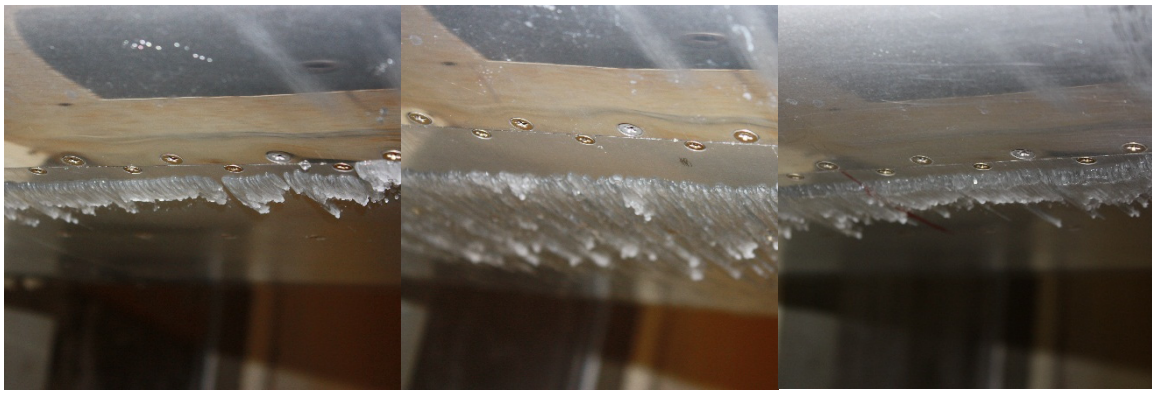

Figure 6.—Warm hold case (a) Reference, (b) Reynolds scaling, and (c) Weber scaling.

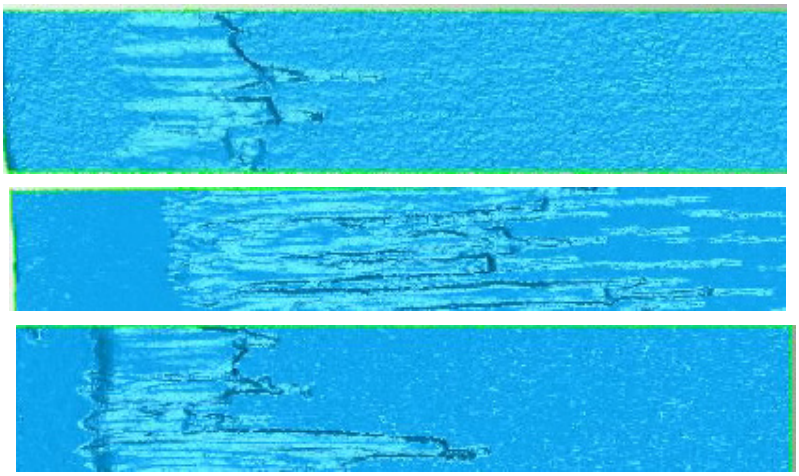

Figure 7.—Scans of impressions of warm hold ice (a) Reference, (b) Reynolds scaled, and (c) Weber scaled.

TABLE 4.—WARM HOLD CASE RESULTS

Flight phase	Alt., ft	V_{tas}, kts	T_{st}, °C	T_t, °C	LWC, g/m^3	MVD, μm	Tau, s	Up ice, in.	Lo ice, in.	Ice mass, g
Wm Hld(ref)	4572	180	–8.7	–4.4	0.53	17.2	420	0.05	---	17
(Re sc)	314	106	–6.2	–4.7	0.83	24.6	420	0.09	---	91
(We sc)	828	180	–8.5	–4.2	0.58	19.9	420	0.11	0.12	29

The airfoil surface temperature data for the Warm Hold case are given in Figure 8. Here, the surface temperatures for the reference and Reynolds number scaled runs matched extremely well for the dry conditions. As in the Descent case, surface temperatures for the dry conditions of the Weber number scaled run are not as well matched even after adjusting IPS settings due to the differing heat transfer. When the model is exposed to icing for this scenario, the surface temperatures vary a little more widely, but are still reasonably close; ±1 °C.

Heated air inlet and outlet temperatures as well as the heat energy input for the reference and scaled conditions are shown in Figure 9. Here again, the data are well matched between the reference and Reynolds number scaled conditions showing that Reynolds number scaling provides a good method of simulation for heat transfer. As expected, the Weber number scaled conditions show a significant increase in heat transfer.

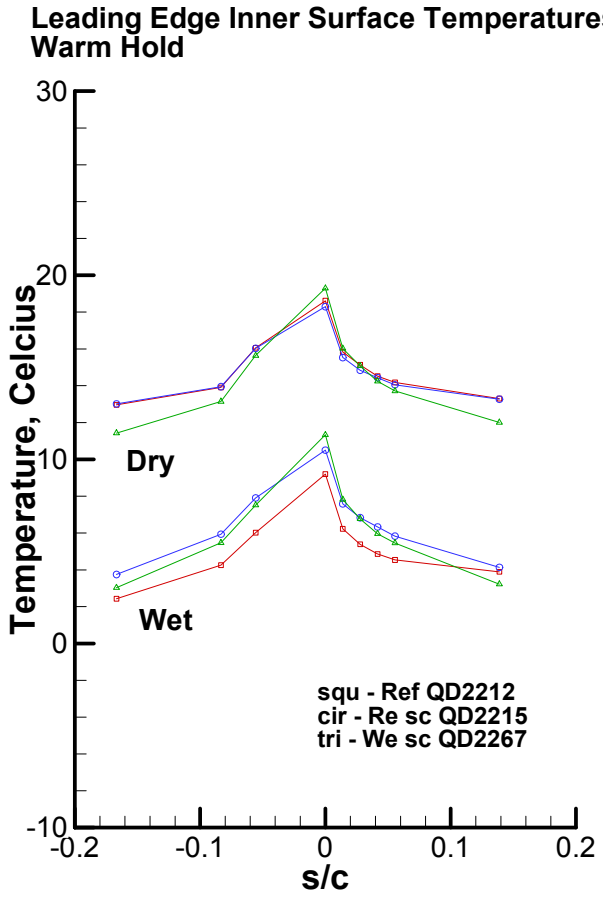

Figure 8.—Warm Hold surface temperatures before (dry) and during (wet) exposure to icing cloud.

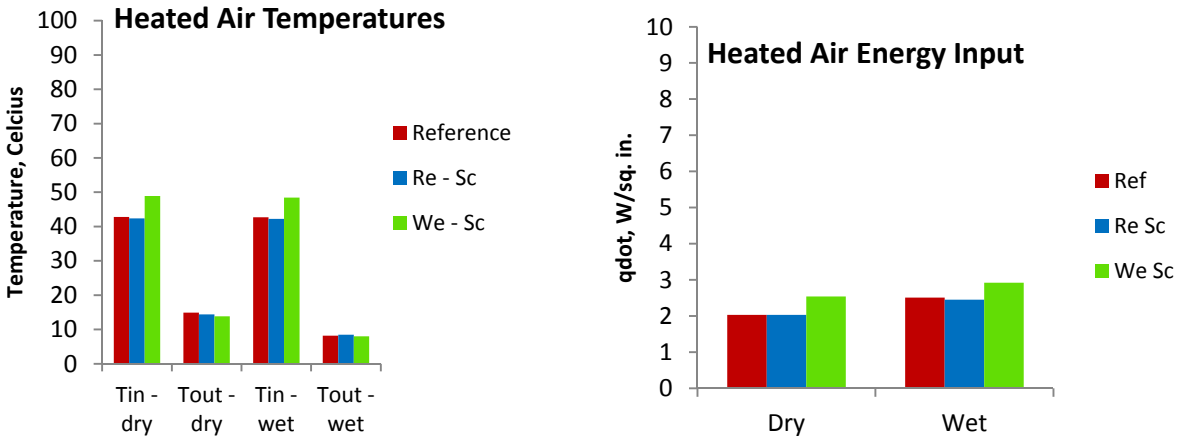

Figure 9.—Warm Hold (a) heated air temperatures and (b) heated air energy input before and during exposure to icing cloud.

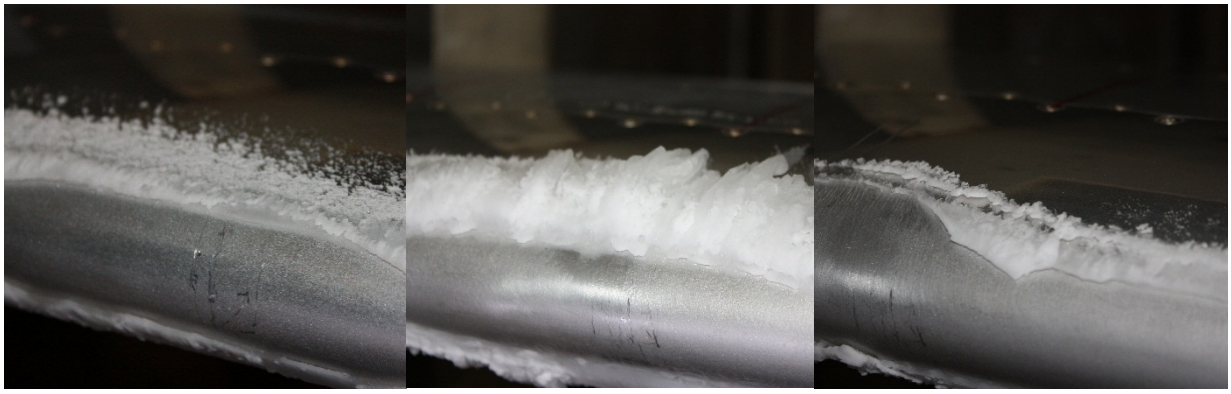

Figure 10.—Cold Hold case: (a) Reference, (b) Reynolds scaling, and (c) Weber scaling with increased surface temperature, ice shed.

Cold Hold Case

Photographs of the ice accreted for the reference and scaled conditions of the Cold Hold case are shown in Figure 10. In this scenario, the reader will note that the runback ice accreted not far from the front of the leading edge where it formed a distinctive ridge. For the Weber number scaled test case, a portion of the ice shed each time the test point was run. Ice would build in a fashion similar to the reference run, but more rapidly, accreting in a forward direction along the surface of the airfoil. The accretion would continue until a section of the ice would shed and be blown downstream. The ice remaining after such a shed is shown in Figure 10(c). It was evident that, for the Weber number scaled case of this Cold Hold scenario, the increased convective cooling by the airstream was causing ice to accrete in a slightly different manner than in the reference case. In an attempt to counter the increased freezing rate, the airfoil surface temperature was increased by approximately 5 °C above that for the reference case. This is referred to as the Weber-II test run. Again, the ice accreted more rapidly than in the reference case and resulted in a portion being shed. The result of this case is shown in the photograph of Figure 10(c). Photographs and ice tracings of the Weber number scaled case, where the surface temperatures were matched to those of the reference condition, were not taken and ice thickness and mass were not recorded.

The ice tracings for the reference, Reynolds number, Weber-II cases are shown in Figure 11. It can be seen that even though the ice accretes more rapidly for the Weber-II scaled case than in the reference case, the resulting ice was much more representative of the reference ice accretion than the ice that was accreted in the Reynolds number scaled case. The measured ice height and mass data for this case are given in Table 5.

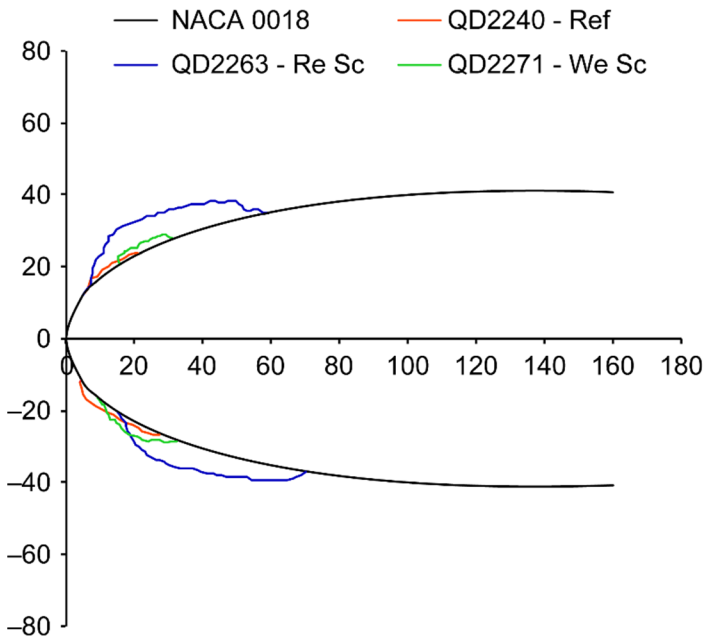

Figure 11.—Cold Hold ice tracings.

TABLE 5.—COLD HOLD

Flight phase	Alt., m	V_{tas}, kts	T_{st}, °C	T_t, °C	LWC, g/m^3	MVD, μm	Tau, s	Up ice, in.	Lo ice, in.	Ice mass, g
Cld Hld(ref)	15000	180	–30.0	–25.6	0.24	17.6	600	0.06	0.09	13
(Re sc)	390	106	–27.5	–26.0	0.41	24.6	600	0.20	0.22	76
(We sc)	869	180	–28.4	–24.1	0.25	19.5	600	-----	-----	--
(We sc-II[a])	781	180	–28.8	–24.6	0.25	19.6	600	0.12	0.14	[b]16

[a]Surface temperature increased above that for reference case.
[b]Ice shed from upper surface.

Model surface temperatures for the Cold Hold scenario are shown in Figure 12. The temperature profiles for the reference, the Reynolds number, as well as both the Weber number and the Weber-II scaled cases are shown. The increase in surface temperatures for the Weber-II scaled case is clearly illustrated in this figure. Figure 13 shows the heated air temperatures and heat energy used by the IPS for each of the four cases.

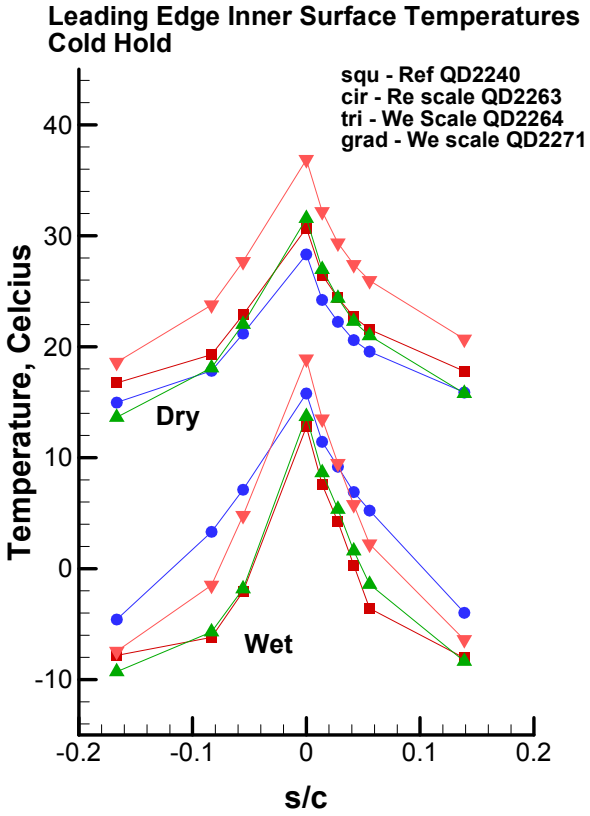

Figure 12.—Cold Hold surface temperatures before (dry) and during (wet) exposure to icing cloud.

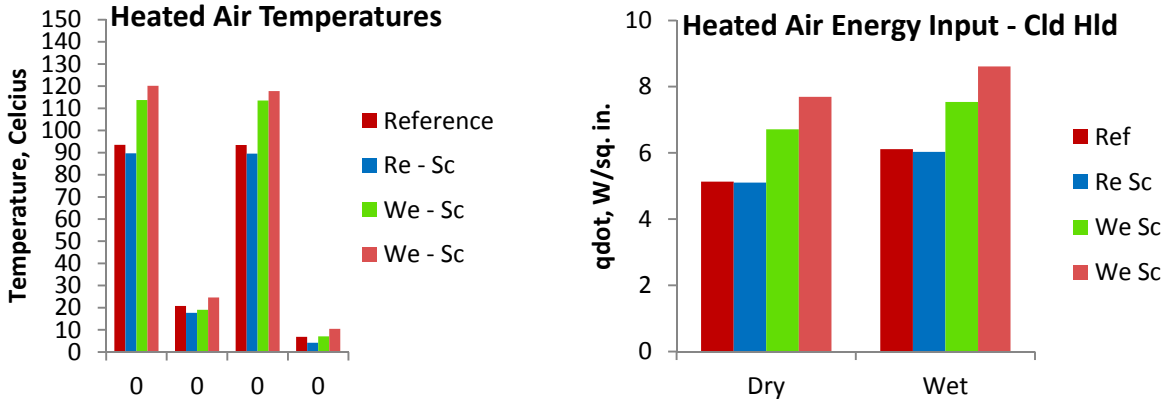

Figure 13.—Cold hold (a) heated air temperatures and (b) heated air energy input before and during exposure to icing cloud.

Time History of Shed Ice

Ice shedding from a model under runback ice conditions is fairly common. It is, however, informative to examine in more detail what is occurring during this process. Figure 14 shows the model surface temperatures at two locations on the model leading edge as a function of time during one of the Cold Hold runs at reference (altitude) conditions. TC1 is located at the foremost point of the nose circle. This is location where the heated air first contacts the airfoil surface, so the surface temperature is highest here. TC10 is located on the upper surface at x = 2.5 in. (6.4 cm) or at x/c of 14 percent along the chord of the model.

Over the first 400 sec of the time history, the heated air temperature was adjusted to obtain the desired leading edge temperature while the tunnel was run at the planned airspeed and temperature. The icing cloud was not operating during this time. The numbers in the figure correspond to the following events:

1. Model comes to steady state under dry air conditions with the IPS operating
2. Icing cloud is turned ON
3. Model leading edge temperature decreases as the supercooled water in the cloud begins to strike the surface and cool it
4. Ice begins to form
5. Ice has formed upstream of TC10's location and creates a boundary layer trip that enhances heat convection and lowers the surface temperature dramatically
6. The surface temperature at TC10 reaches a steady state condition
7. Ice has accreted forward over much of the leading edge and is now providing a layer of insulation from the tunnel flow. The surface temperature under the ice is now increasing as it is warmed by the heated air flowing over its inner surface.
8. The warming airfoil surface under the ice has debonded and or weakened the ice so as to precipitate a shed. The shed ice now exposes a larger surface of the airfoil to the tunnel flow such that its temperature drops rapidly.
9. Ice is starting to build again as the heated air is turned off just prior to ending the test run.

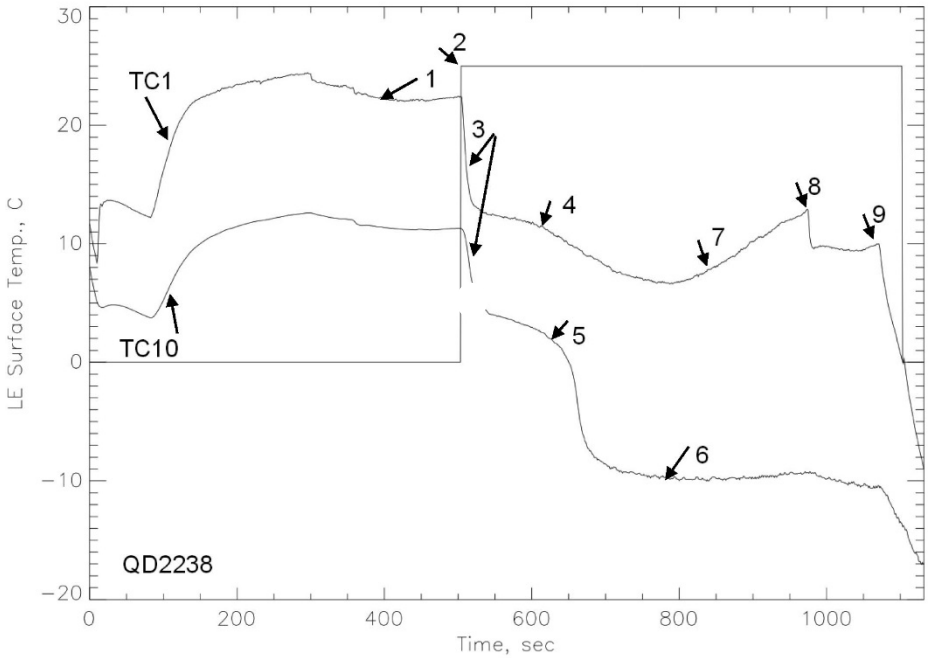

Figure 14.—Time history of leading edge temperatures during a test run with an ice shed event.

Discussion

As was shown in the initial test campaign, the close matching of airfoil surface temperatures, heated air inlet and outlet temperatures, and energy use rates between the reference and Reynolds number scaled conditions showed that this scaling method works well in matching the heat transfer between altitude and ground level conditions. The matching of surface temperatures between reference and Weber number scaled cases was done deliberately by adjusting the operation of the thermal IPS to obtain such matching. The associated increase in heat transfer from the IPS was needed to account for the increase in convective cooling from the airstream at Weber number scaled conditions. Matching surface temperatures is a necessary, but not necessarily sufficient, condition for ice to accrete in a fashion similar to that in the reference conditions.

The actual amount and location of the ice accreted was much better approximated by the Weber number scaling method than the Reynolds number scaling method. This can be seen in the ice tracings, the photographs, and in the impressions of the ice taken during the tests and shown in the figures of this report. Comparisons of the amounts of ice accreted for the reference and scaled cases for each of the icing flight scenarios are shown in Figure 15. While the amount of ice is not identically matched to the reference value by the Weber number method, it is much better matched than with the Reynolds number scaling.

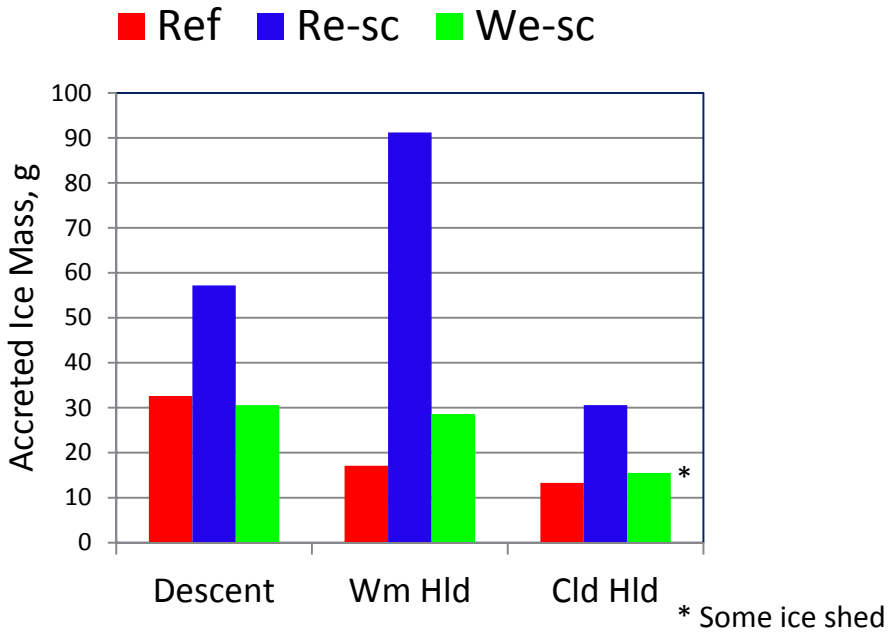

Figure 15.—Comparison of ice mass accreted for reference, Reynolds number, and Weber number scaled cases for each of the icing flight scenarios.

Closing Remarks

This study was the second in a series designed to better understand the effects of altitude on thermal IPS performance. These studies have provided the first publicly available data on the effects of altitude on thermal IPS operation. They have shown that Reynolds number scaling is effective in simulating heat transfer occurring at altitude conditions, but it does not simulate mass transfer (i.e., runback ice accretions) well. The current study showed that Weber number scaling results in ice accretions much more similar in size, shape, location and mass to those formed at altitude conditions than Reynolds number scaling alone does. The increased heat transfer occurring at Weber number scaling conditions does, however, have an effect on the runback ice formation, particularly at low air temperatures. The new, two-step altitude scaling method proposed and evaluated in this report provides a way of evaluating both the heat transfer and mass transfer performance of a thermal ice protection system that does not rely on the application of empirical correction factors, but instead relies on the straightforward application of the primary physics involved.

References

1. SAE AIR6440, "Icing Tunnel Tests for Thermal Ice Protection Systems," SAE AC-9C Aircraft Icing Technology Committee, June 2014.
2. Anderson, D.N., "Manual of Scaling Methods," NASA/CR—2004-212875, 2004.
3. Addy, H.E., Oleskiw, M., Broeren, A.P., Orchard, D., "A Study of the Effects of Altitude on Thermal Ice Protection System Performance," AIAA–2013–2934, NASA/TM—2013-216559.
4. Incropera, F. and DeWitt, D.P., "Fundamentals of Heat and Mass Transfer," p. 349, 1990.
5. Ishii, M. and Grolmes, M.A., "Inception Criteria for Droplet Entrainment in Two-Phase Concurrent Film Flow," AIChE Journal Vol. 21, No. 2, March 1975.
6. Kim, B.H., Peterson, G.P., and Kihm, K.D., "Analytical and Experimental Investigation of Entrainment in Capillary Pumped Wicking Structures," Journal of Energy Resources Technology, Transactions of the ASME, Vol. 115, p. 278–286, December 1993.
7. Audouin, A., Ern, P., and Charru, F., "Droplet Entrainment from a Single Wave Propagating in a Stratified Air-Water Pipe Flow," (2013) In: 25th European Conference on Liquid Atomization and Spray Systems, 01 September 2013–04 September 2013 (Chania, Greece).
8. Olsen, W., and Walker, E., "Experimental Evidence for Modifying the Current Physical Model for Ice Accretion on Aircraft Surfaces," NASA TM-87184, January 1997.
9. Kind, R.J., and Oleskiw, M.M., "Experimental Assessment of a Water-Film-Thickness Weber Number for Scaling of Glaze Icing," AIAA–2001–0836, January 2001.
10. Feo, A., "Similarity of Water Film Weber Number and Film Thickness in Icing Scaling," AE/TNO/4420/264/INTA/014, Instituto Nacional de Tecnica Aeroespacial, October 2001.
11. Oleskiw, M.M., Hyde, F.H., and Penna, P.J., "In-Flight Icing Simulation Capabilities of NRC's Altitude Icing Wind Tunnel," AIAA–2001–0094, 2001.